

# Theoretically study of the magnetic and transport properties on carbon nanotubes

D. RACOLTA\*, C. ANDRONACHE

Technical University of Cluj Napoca, North University Center of Baia Mare, Str. Victoriei 76 430122, Baia Mare, Romania

In this paper we one deals with the theoretically study of the magnetic and transport properties on carbon nanotubes. To this aim one resorts to a tight binding model by accounting for a single  $\pi$ -band, in which spin degrees of freedom have also been accounted for. We show that the application of an external magnetic field produces changes in transport properties of carbon nanotubes. When the applied magnetic field is parallel to the tube axis, one gets faced with the implementation of the well-known Aharonov-Bohm (AB) quantum phase which is relevant for applications in mesoscopic devices. We found that the AB-oscillations in carbon nanotubes with zig-zag boundary conditions are characterized by integer ( $\phi_0$ ) and ( $\phi_0/2$ ) magnetic-flux periods. This result leads to sawtooth-type oscillations relying on the parity of the electron number. In the presence of a transversal magnetic field we found a halving of the Fermi velocity and an increase of the density of states (DOS) in metallic nanotubes, which is reflected in conductance measurements, while the energy gap is suppressed in semiconducting nanotubes.

(Received October 20, 2016; accepted October 10, 2017)

*Keywords:* Carbon nanotubes, Persistent currents, Aharonov-Bohm effect

## 1. Introduction

Theoretical investigations concerning persistent currents and AB effect in mesoscopic structures based on graphene and carbon nanotubes, in the presence of magnetic field have received much attention during the last years [1, 2]. This opens the way for technological applications in nanodevices [3, 4].

Graphene (a monolayer graphite) is a material consisting of an individual layer of carbon atoms arranged in a two dimensional hexagonal lattice [5-7]. The energy band structure and structural properties of graphene and carbon nanotubes are calculated using a tight binding model based on the nearest neighbor interaction which includes one  $p_z$  orbital per carbon atom.

The discovery of carbon nanotubes [8] which are basically rolled up sheets of graphite hexagonal networks of carbon atoms forming tubes opened a new field of research in the physics at nanoscales [9]. Depending on the orientation and the direction of the edges leads to three types of nanotubes called armchair, zigzag and chiral nanotubes. The electronic structure of carbon nanotubes can be derived from the electronic structure of graphene [10], after introducing periodic boundary conditions due to the cylindrical geometry of the tube. This results in a set of 1D energy dispersion relations which are cross-sections of those for 2D graphene. All the armchair nanotube ( $m-n=0$ ), exhibit a metallic character. For the zigzag nanotube, the character depends on chirality: if ( $m-n$ ) is a multiple of 3, there is no gap in the energy spectrum, showing

metallic character, if ( $m-n$ ) is not a multiple of 3, the gap is non-zero so that the character is semiconducting.

In the presence of the magnetic flux we have to account for similarities with small mesoscopic metallic rings. Accordingly, the Aharonov-Bohm oscillations and the persistent currents exhibit alternately integer periods ( $\phi_0$ ) and halved periods ( $\phi_0/2$ ). Recall that the magnetic flux quantum is given by  $\phi_0=hc/e$ . The density of states (DOS) depends of the size nanotube, which is reflected in conductance measurements. Those with small diameters have a large gap and those with large diameters have a small gap and begin to behave like graphene at high temperatures.

## 2. Model and formulation

The hexagonal lattice of graphene is characterized by lattice vectors like  $a_1 = (\sqrt{3}a/2, a/2)$  and  $a_2 = (\sqrt{3}a/2, -a/2)$ , where  $a = \sqrt{3}a_0$ ,  $a_0 = 1.42\text{\AA}$  is the C-C distance. The points  $K$  and  $K'$  situated at the corners of the first Brillouin zone of graphene are named Dirac points and their positions in momentum space are given by [11],  $K = (2\pi/3a, 2\pi/3\sqrt{3}a)$ ,  $K' = (2\pi/3a, -2\pi/3\sqrt{3}a)$ .

The well known energy bands for graphene [12] derived using tight binding hamiltonian are [13]

$$E(k) = \pm t \sqrt{1 + 4 \cos^2\left(\frac{k_y a}{2}\right) + 4 \cos\left(\frac{k_y a}{2}\right) \cos\left(\frac{\sqrt{3} k_x a}{2}\right)}, \quad (1)$$

Tight binding model shows, that graphene has full valence band and empty conduction band, while the top of the valence band has exactly the same energy as the bottom of the conduction band. Therefore graphene is called a zero band-gap semiconductor or semimetal, since electronic properties get ranged between the ones of metal and semiconductors. The energy bands of graphene at low energies are described by a 2D Dirac-like equation with linear dispersion near  $K/K'$ -points in  $k$  space.

The one-dimensional band structure of carbon nanotube is obtained by quantization the two-dimensional band structure of the graphene sheet along the circumferential direction of the nanotube [14]. The chiral vector

$$C_h = ma_1 + na_2, \quad (2)$$

determines the circumference of the carbon nanotube ( $m, n$  are integers). Eliminating  $k_x$ , or  $k_y$  by using the periodic boundary condition,

$$C_h \cdot k = 2\pi \cdot l, \quad (3)$$

where  $l$  is an integer, we get 1D energy bands for general chiral structures. We can define a quantization rule [15],

$$\frac{\sqrt{3}a}{2}(m+n)k_x + \frac{a}{2}(m-n)k_y = 2\pi l, \quad (4)$$

so, that:

$$k_x = \frac{4\pi l}{\sqrt{3}a(m+n)} + \frac{n-m}{\sqrt{3}(m+n)}k_y. \quad (5)$$

The energy dispersion relation for the case  $m=n$ , armchair nanotube ( $n, n$ ), is obtained by substituting of the discrete allowed values for  $k_x$  into Eq. 1. In this case, all the armchair nanotubes ( $m=n=0$ ), present a metallic character.

$$E_l(k) = \pm t \sqrt{1 + 4 \cos^2 \left( \frac{\sqrt{3}k_y}{2} a_0 \right) \pm 4 \cos \left( \frac{\sqrt{3}k_y}{2} a_0 \right) \cos \left( \frac{l\pi}{n} \right)}, \quad (6)$$

where,  $-\pi < ka < \pi$ . Thus due the periodic boundary condition along the  $x$  direction, the wavevector component  $k_x$  is quantized,

$$k_x = l \frac{2\pi}{n\sqrt{3}a}. \quad (7)$$

Next, we consider the case  $m=0$ , the zigzag nanotube ( $n, 0$ ) or ( $n, -n$ ) which gives a simple quantization rule in the form,

$$k_y = l \frac{2\pi}{na}. \quad (8)$$

So,

$$E_l(k) = \pm t \sqrt{1 + 4 \cos^2 \left( \frac{l\pi}{n} \right) \pm 4 \cos \left( \frac{l\pi}{n} \right) \cos \left( \frac{3}{2} k_x a_0 \right)}, \quad (9)$$

where,  $-\pi/3 < k_x a_0 < \pi/3$ . We obtain that just 1/3 of the possible nanotubes are metallic when the condition  $m-n$  multiple of 3 is fulfilled.

### 3. Results

In this paper we describe the oscillations of magnetization and persistent currents when a magnetic field is applied along the axis of the nanotube (Aharonov Bohm effect (AB)). The AB effect reflects the dependence of the phase of the electron wave on the magnetic field.

We describe the AB oscillations and the persistent currents only for the case with zigzag boundary condition, based on an extended tight-binding model, now by using a single  $\pi$ - band, which are dependent on the magnetic flux  $\Phi$ , like the case of mesoscopic metallic rings [16].

The magnetic flux is given by:

$$\phi = \int \vec{B} \cdot d\vec{S}, \quad (10)$$

where  $S = \pi R^2$  is the area, with  $R$  being the radius of the carbon nanotube.

The expression of the magnetic phase factor [17, 18] is:

$$\theta_{i,j} = \frac{2\pi}{\phi_0} \int_i^j \vec{A} \cdot d\vec{l}, \quad (11)$$

where,  $\vec{A}$  denotes the vector potential associated with the applied perpendicular magnetic field  $B$ .

The wave function acquires an additional phase factor. This leads to the modification of the wave number  $k$ , like:

$$k'_y = k_y + \frac{\phi}{|C_h| \phi_0}. \quad (12)$$

Fixing the number of electrons the total magnetization is given in terms of the sum over states [19]

$$M = - \frac{dE_{tot}}{dB}. \quad (13)$$

The magnetic field induces a persistent current along the transversal direction of the nanotube

$$I = -c \frac{dE_{tot}}{d\phi}, \quad (14)$$

in which,  $E_{tot}$  denotes the total energy, namely

$$E_{tot} = \sum_{i,\sigma} \varepsilon_i(B). \quad (15)$$

One sees that  $E_{tot}$  is given by the sum over all occupied single-particle (noninteracting electrons) energies, while the index  $\sigma$  runs over spins. In calculating  $E_{tot}$ , only the single-particle tight binding energies with  $\varepsilon_{i(B)} > 0$  are considered [20].

The AB patterns exhibited by the magnetization curves display a well developed (although apparently not perfect) alternation pattern between integer periods ( $\phi_0$ ) and halved periods ( $\phi_0/2$ ), as long as the highest occupied state lies in the interior of the sixfold energy band. The  $\phi_0/2$  period reflects the zigzag nature of related states. Moreover, period doubling effects in the oscillations of persistent currents in discretized AB-rings have also been discussed [21].

In Fig. 1-3, we displayed the magnetization curves with the number of electrons ranging from  $N=57-72$ . The AB patterns can be described as an odd even effect due to a two-electron alternation as a function of  $N$  [22], where  $N=12i+N_0$  ( $i=1,2,3,\dots$  and  $N_0=1,2,\dots,6$ ).

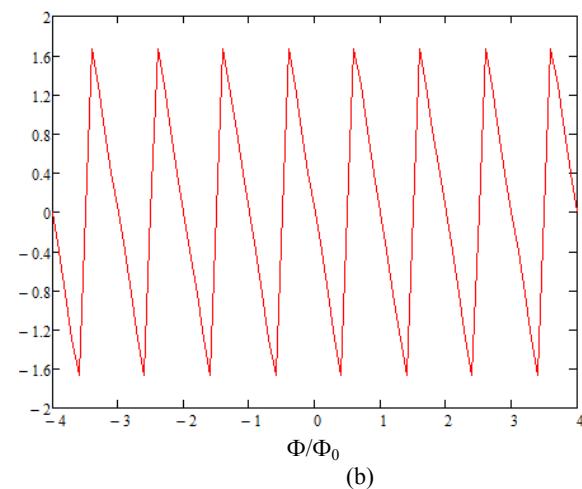
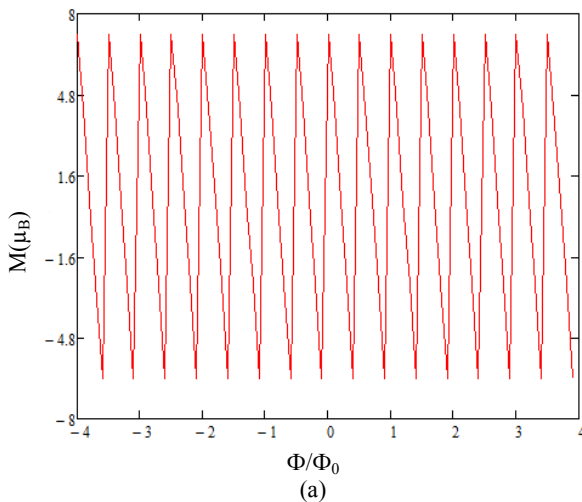


Fig. 1. Magnetization as a function of the magnetic flux  $\Phi$  (spin is included). (a)  $N=63$ ; shifted halved-period sawtooth pattern; (b)  $N=64$ ; shifted sawtooth

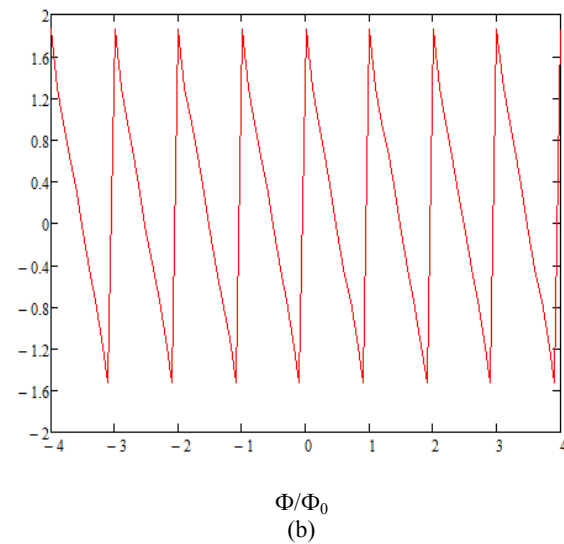
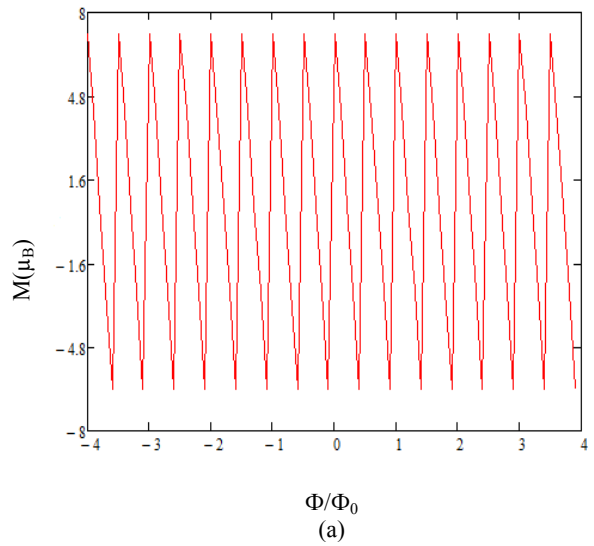
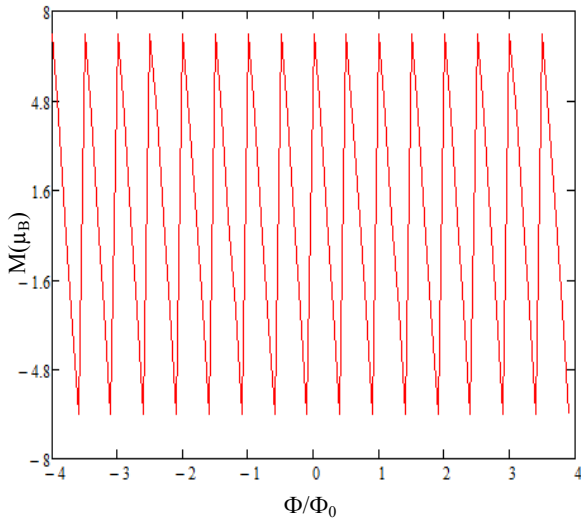
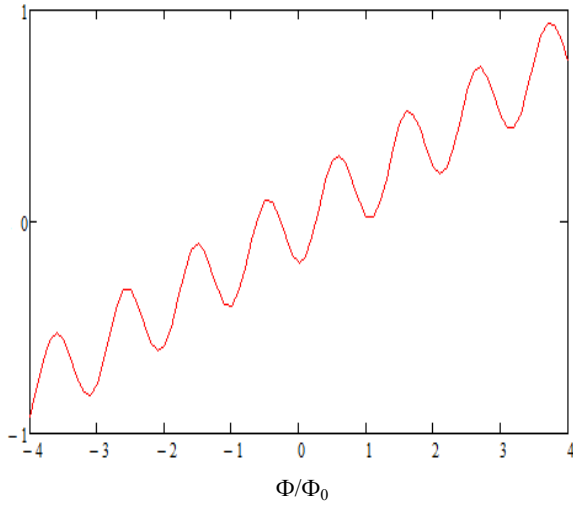


Fig. 2. Magnetization as a function of the magnetic flux  $\Phi$  (spin is included). (a)  $N=65$ ; shifted halved-period sawtooth pattern, (b)  $N=66$ ; sawtooth pattern

As can be seen in Fig. 1-3, we found nontrivial odd-even parity effects in the flux-dependence of the total current, which concerns both the period of oscillations as well as the corresponding magnitudes. In the studied range ( $N=60$  to  $N=72$ ), the magnetization curves exhibit an odd-even effect associated with the alternation between a whole-period sawtooth oscillation and a halved-period sawtooth pattern as shown in Fig.1-3(a). The last curve ( $N=72$ ) showing a full-period with rounded-sawtooth behavior (Fig. 3(b)) and the two curves for the bottom level ( $N=61$ ,  $N=62$ ), exhibit both a full-period sawtooth behavior.



(a)



(b)

Fig. 3. Magnetization as a function of the magnetic flux  $\Phi$  (spin is included). (a)  $N=69$ ; shifted halved-period sawtooth pattern; (b)  $N=72$ ; rounded sawtooth

The density of states (DOS) evolution from graphite to a nanotube is based on size quantization effects arise when the dimensions are reduced [23].

The DOS represents the number of energy eigenstates per unit energy

$$D(E) = \frac{d}{dE} N(E), \quad (16)$$

and depends on  $E(\vec{k})$ . The energy levels can be described by a parabolic dispersion relation with some effective mass  $m^*$ :

$$E(\vec{k}) = E_c + \frac{\hbar^2 k^2}{2m^*}. \quad (17)$$

The allowed states in  $k$ -space are distributed with a density of  $(L/2\pi)$  per unit  $k$ , where  $L$  stands for the length of nanotube. So, the total number of allowed states is given by:

$$N(k) = \frac{L}{2\pi} 2k = \frac{kL}{\pi}. \quad (18)$$

The total number of states:

$$N(E) = \frac{L [2m^*(E - E_c)]^{1/2}}{\pi \hbar}, \quad (19)$$

is in accord with Eq. 17.

Considering the Eq.9, for the energy dispersion relation, the DOS expression for a zigzag nanotube becomes:

$$D(E) = \sum_l \frac{L}{\pi a t} \frac{E}{\sqrt{E^2 - E_l^2}}. \quad (20)$$

Analytically it is possible to replace the  $l$ -summation by an integral. Then the DOS for zigzag nanotubes is given by:

$$D(E) \approx \int_0^l 2dl \frac{2L}{\pi a t} \frac{|E|}{\sqrt{E^2 - E_l^2}}. \quad (21)$$

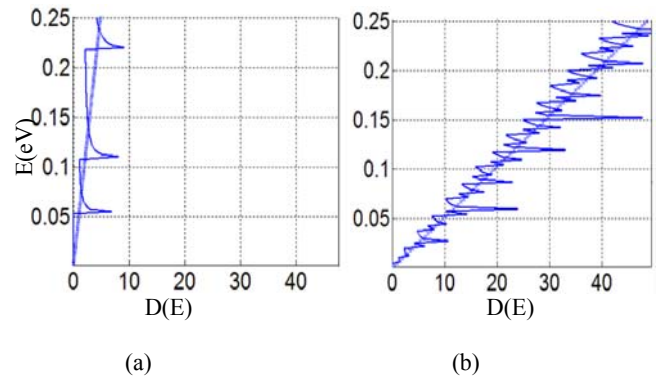


Fig. 4. Density of states  $D(E)$  for a zigzag nanotube (solid line) compared with graphite (crosses line). (a)  $n = 150$  (corresponding to  $d = 11.55$  nm); (b)  $n = 1500$  ( $d = 115.5$  nm).

The semiconducting DOS gap depends on the size of the nanotube. We note that the smaller nanotube has a DOS that is distinctly different from graphite. But the larger nanotube is less distinguishable. Those with small diameters have a large gap and those with large diameters have a small gap (Fig. 4). This is especially true at high temperatures, when nanotubes with a large diameter begin to look like graphene. Recent experiments have confirmed such theoretical predictions.

#### 4. Conclusions

We obtained the electronic structure of nanotubes from the electronic structure of graphene by calculating how rolling of the sheet affects the electronic structure.

We succeeded to prove the universality of integer ( $hc/e$ ) and half-integer ( $hc/2e$ ) values for the period of the AB oscillations as a function of the magnetic flux, in consonance with the case of mesoscopic metal rings. The AB effect is a fundamental phenomenon of quantum interference related on the transmission of particles through a closed loop pierced by a magnetic flux. Odd-even (in the number of Dirac electrons,  $N$ ) sequences sawtooth-type patterns relating to the halving of the period have also been found.

We demonstrated that the semiconducting DOS gap depends on the size of nanotube. DOS experimental measurements show in addition sharp peaks that are characteristic signatures of the one-dimensional (1D) nature of the conductance. We have to remark that the 1D nature of the electron system in nanotubes has been confirmed by resonant Raman scattering experiments.

#### Acknowledgements

The authors thanks Prof. E. Papp for useful discussions and remain indebted to the late Prof. C. Micu for her supports and encouragements.

#### References

- [1] S. Roche, G. Dresselhaus, M. S. Dresselhaus, R. Saito, Phys. Rev. B **62**, 16092 (2000).
- [2] P. Recher, B. Trauzettel, A. Rycerz, Y. M. Blanter, C. W. J. Beenakker, A. F. Morpurgo, Phys. Rev. B **76**, 235404 (2007).
- [3] A. Fujiwara, K. Tomiyama, H. Suematsu, M. Yumura, K. Uchida, Phys. Rev. B **60**, 13492 (1999).
- [4] N. Kim, J. Kim, J.-O Lee, K. Kang, K.-H. Yoo, J. W. Park, H.-W. Lee, J.-J. Kim, J. Phys. Soc. Jpn. **70**, 789 (2001).
- [5] K. S. Novoselov, A. K. Geim, S. V. Morozov, D. Jiang, Y. Zhang, S. V. Dubonos, I. V. Grigorieva, A. A. Firsov, Science **306**, 666 (2004).
- [6] C. Berger, Z. Song, X. Li, X. Wu, N. Brown, C. Naud, D. Mayou, T. Li, J. Hass, A. N. Marchenkov, E. H. Conrad, P. N. First, W. A. de Heer Science **312**, 1191 (2006).
- [7] S. B. Sinnott, R. Andrews, Critical Reviews in Solid State and Materials Sciences **26**, 145 (2001).
- [8] R. Saito G. Dresselhaus, M. S. Dresselhaus, Physical Properties of Carbon Nanotubes, Imperial College Press, London 1998, p. 259.
- [9] P.R. Wallace, Physical Review **17**, 9 (1947).
- [10] S. Iijima, Nature **354**, 56 (1991).
- [11] P.L. McEuen, Nature **393**, 15 (1998).
- [12] V. Popov, Materials Science and Engineering **43**(3), 61 (2004).
- [13] S. Belluci (ed), Physical Properties of Ceramic and Carbon Nanoscale Structures, The INFN Lectures, Vol. II, Springer-Verlag Berlin Heidelberg (2011).
- [14] D. Racolta, C. Andronache, D. Todoran, R. Todoran, Rom. J. Phys. **61**, 992 (2016)
- [15] J. Schelter, P. Recher, B. Trauzettel, Solid State Communications **152**, 1411 (2012).
- [16] D. Racolta, C. Micu, Analele Univ. de Vest **57**, 52 (2013).
- [17] E. Papp, C. Micu, Low dimensional nanoscale systems on discrete spaces, World Scientific, Singapore, (2007).
- [18] G. Ardelean, Appl. Math. Comput. **218**, 88 (2011)
- [19] A. H. Castro Neto, F. Guinea, N. M. R. Peres, K. S. Novoselov, A. K. Geim, Reviews of Modern Physics **81**, 109 (2009).
- [20] P. Recher, B. Trauzettel, A. Rycerz, Ya. M. Blanter, C. W. J. Beenakker, A. F. Morpurgo, Phys. Rev. B **76**, 235404 (2007).
- [21] E. Pap, C. Micu, D. Racolta, Physica E **36**, 178 (2007).
- [22] I. Romanovsky, C. Yannouleas, U. Landman, Phys. Rev. B **85**, 165434 (2012).
- [23] S. Datta, Quantum Transport: Atom to Transistor, Cambridge University Press, New York (2005).

\*Corresponding author: daniaracolta@yahoo.com